Analysis of Converter Process Variables from Exhaust Gas*

*By Takeshi TAKAWA,** Katsumi KATAYAMA,** Ken KATOHGI*** and Takashi KURIBAYASHI****

Synopsis

A new mathematical model of which the dynamic equations of material and heat balance are combined with the exhaust gas information obtained by mass-spectrometer has been established for the improvement of the end point control of BOF.

The outline of the model calculation is as follows:

(1) From the amounts of oxygen and submaterials charged into BOF and the composition and flow rate of the gas exhausted from BOF, the amounts of oxygen consumed on the surface of cavity of molten steel and of oxygen consumed by decarburization can be determined.

(2) The transition of composition and temperature of steel bath can be estimated from the amount of oxygen calculated by the above way on the basis of model of reaction theory.

At No. 1 BOF shop in Wakayama Steel Works, the model is now being used as the guide of the operation and contributes to the reduction of reblow ratio.

Key words: basic oxygen steelmaking; modeling; mathematical model; end point control; indirect measurement; converter process; exhaust gas information; material and heat balance; mass-spectrometer; reaction theory; transition of composition and temperature.

I. Introduction

The most important subject in the BOF steelmaking process is to predict the steel composition and temperature at the end point of blowing. For this purpose, development works on the computer control of BOF process had been started in early 1960's at home and abroad. In Japan a method of controlling the carbon content and temperature at the end point of blowing has almost been established by the combination of sub-lance measurement in the final stage of blowing with a simple control model.[1-3]

Muchi and Moriyama[4] devised a mathematical model of which the transition of composition and temperature of steel bath can be calculated from the dynamic equations of material and heat balance derived from metallurgical reaction theory. Taguchi *et al.*[5] also reported the control results obtained by the mathematical model of the same sort.

Tanaka *et al.*[6] studied the method of calculating the amount of oxygen remaining in the furnace every moment on the basis of the information of exhaust gas, and found that the degree of scatter in the phosphorus and manganese contents at the end point can be reduced if the amount of remaining oxygen is controlled so as to be in a suitable range. Iida *et al.*[7] established a control technique for slag formation by the adjustment of lance height and flow rate of oxygen on the basis of the measured result of lance vibration. Recently a method of estimating the phosphorus content at the end point from the oxygen content measured by an oxygen sensor has been reported.[8] A method of estimating the phosphorus and manganese contents of steel bath during blowing and using the estimation for end point control, is not fully established for the practical application.

In this paper, the reaction model proposed by Muchi and Moriyama[4] has been modified so as to be suitable for the on-line application by combining the model with the information of gas exhausted from BOF. The transition of composition including the phosphorus and manganese contents and temperature of steel bath during blowing can be estimated through the on-line application of this model at No. 1 BOF shop in Wakayama Steel Works.[9] This paper deals with the general features of the mathematical model and the results of practical application.

II Construction of the Mathematical Model

1. Basic Conception of the Mathematical Inferential Model

Complicating reactions such as the reactions between gas and metal on the surface of cavity of molten steel and the reactions between slag and metal may take place in the furnace. Although the exact formulation of this process is hardly made, it is possible to make a simplified model which is suitable for the practical application.

In the current work, the reaction model proposed by Muchi and Moriyama[4] has been modified so as to be applicable to the actual operation and to be used as an accurate mathematical model for the indirect measurement through the exhaust gas information obtained by mass-spectrometer.

Main points of the modification are as follows:

(1) Muchi and Moriyama[4] calculated the average time of the molar flow rate of oxygen absorbed per unit surface area of cavity of molten steel and the surface area of cavity, and thereafter the calculated the amount of effective oxygen which is consumed by oxidation only on the surface of cavity out of oxygen supplied into the furnace as the product of the molar flow rate and the surface area. In this paper, the

* Originally published in *Tetsu-to-Hagané*, **73** (1987), 844, in Japanese; formerly presented to the 105th ISIJ Meeting, April 1983, S205, at The University of Tokyo in Tokyo. English version received on June 15, 1987; accepted in the final form on September 11, 1987.

** System Engineering Division, Sumitomo Metal Industries, Ltd., Nishinagasu-Hondori, Amagasaki 660.

*** Wakayama Steel Works, Sumitomo Metal Industries, Ltd., Minato, Wakayama 640.

**** Kashima Steel Works, Sumitomo Metal Industries, Ltd., Oaza Hikari, Kashima-cho, Kashima-gun, Ibaraki Prcf. 314.

amount of effective oxygen and the amount of oxygen consumed by decarburization are calculated on the basis of the information of the gas exhausted from the furnace as a result of reactions during blowing to simplify the model and to improve the accuracy.

(2) Muchi and Moriyama[4] estimated the change in heat energy of metal, on the assumption that the temperatures of metal and slag are the same. In the actual operation, the temperature of slag tends to be higher than that of metal. In this paper, it is assumed that the heat energies such as the heats of reactions and dissolution are distributed to the metal and slag phases in a fixed proportion, differing from the assumption adopted by Muchi and Moriyama.[4] The heat of oxidation of CO gas in the furnace, which is neglected in the model proposed by Muchi and Moriyama,[4] is also considered in the model.

(3) In addition to carbon, silicon, manganese and phosphorus are chosen as the elements which move into the metal phase from scrap and cold metal by dissolution.

(4) The adaptive modification of parameters in the model is made to deal with the variation of operational condition in the on-line application.

The amount of effective oxygen and the amount of oxygen consumed by decarburization can be calculated on the basis of the information on the amounts of blown oxygen and charged submaterials, the composition and the flow rate of exhaust gas during blowing as shown in Fig. 1. The transition of composition and temperature of steel bath can be calculated from the amount of oxygen calculated by the above way on the basis of the model of reaction theory.

2. *Estimation of the Amount of Effective Oxygen*

Figure 2 shows the gas flow during blowing. The amount of air absorbed from the throat of furnace and the amount of ineffective oxygen consumed by oxidation of CO gas in the furnace can be estimated on the basis of the information on the exhaust gas. The amounts of absorbed air and CO_2 gas produced in the furnace can be calculated by the following equations.

$$V_{AIR} = \frac{100}{79} V^{EX}_{N_2} \quad \text{.....(1)}$$

where, V_{AIR}: amount of absorbed air (Nm^3/h)
$V^{EX}_{N_2}$: amount of N_2 in the exhaust gas (Nm^3/h)

$$V^{F}_{CO_2} = V^{EX}_{CO_2} - \left(\frac{21}{100} \cdot V_{AIR} - V^{EX}_{O_2}\right) \times 2 \quad \text{.....(2)}$$

where, $V^{F}_{CO_2}$: amount of CO_2 produced in the furnace (Nm^3/h)
$V^{EX}_{CO_2}$: amount of CO_2 in the exhaust gas (Nm^3/h)

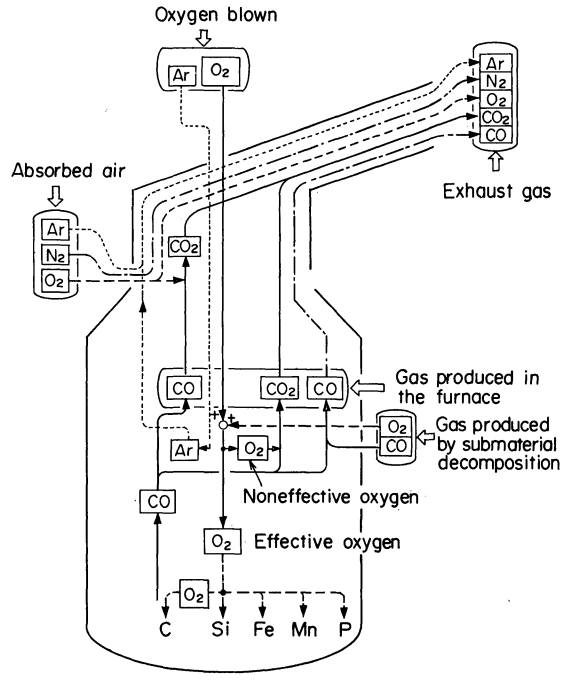

Fig. 2. Gas flow in the furnace.

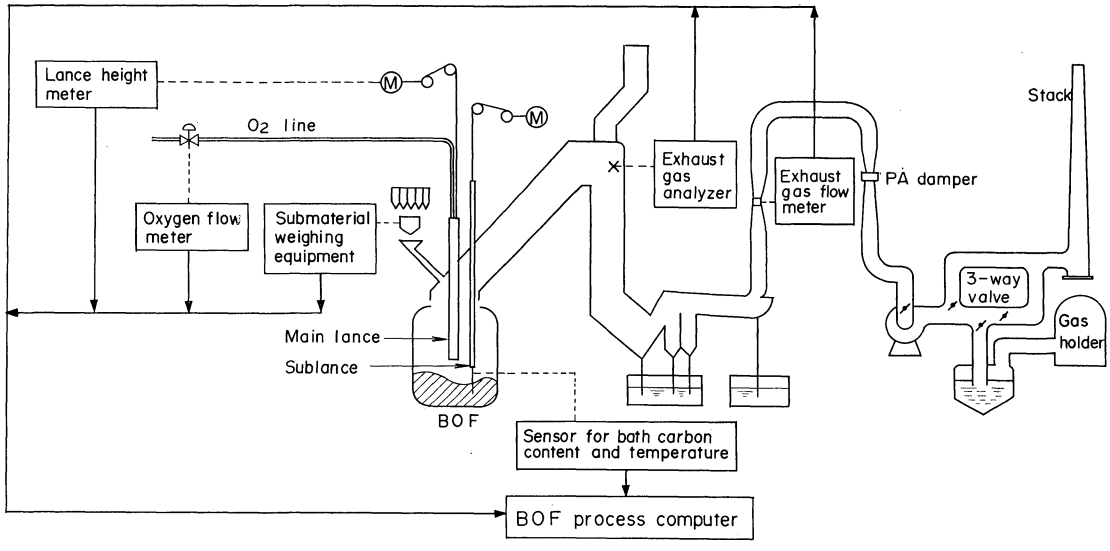

Fig. 1. Measurement system for the model calculation with the exhaust gas information.

$V_{O_2}^{EX}$: amount of O_2 in the exhaust gas (Nm^3/h)

The amount of each gas in the exhaust gas of the above equations is obtained as a product of the flow rate and the concentration of exhaust gas. In this case, the delay of analysis should be taken into consideration for the concentration of exhaust gas. It is confirmed that the delay time is about 20 s by the experiment in which the time required for blown oxygen to show the effect on the concentration of CO in the exhaust gas is measured.

The amounts of ineffective oxygen and effective oxygen are expressed by Eqs. (3) and (4).

$$V_{O_2}^{LOSS} = V_{CO_2}^{F}/2 \quad \text{.....(3)}$$

where, $V_{O_2}^{LOSS}$: amount of ineffective oxygen (Nm^3/h)

$$V_{O_2}^{EFF} = V_{O_2} - V_{O_2}^{LOSS} \quad \text{.....(4)}$$

where, $V_{O_2}^{EFF}$: amount of effective oxygen (Nm^3/h)

V_{O_2}: amount of supplied oxygen (Nm^3/h)

The amount of CO produced by decarburization on the surface of cavity can be expressed by Eq. (5) by the use of the amounts of CO and CO_2 in the exhaust gas.

$$V_{CO}^{CAV} = V_{CO}^{EX} + V_{CO_2}^{EX} - V_{CO}^{SUB} \quad \text{.....(5)}$$

where, V_{CO}^{CAV}: amount of CO produced on the surface of cavity (Nm^3/h)

V_{CO}^{EX}: amount of CO in the exhaust gas (Nm^3/h)

V_{CO}^{SUB}: amount of CO supplied by submaterials (Nm^3/h)

The amount of oxygen consumed by decarburization out of effective oxygen, $V_{O_2}^{DEC}$, is expressed by Eq. (6).

$$V_{O_2}^{DEC} = V_{CO}^{CAV}/2 \quad \text{.....(6)}$$

Figure 3 shows the estimated amounts of absorbed air, CO_2 produced in the furnace and effective oxygen. The amount of ineffective oxygen begins to decrease at about 6 min after the start of blowing as shown in Fig. 3. A clear explanation of this phenomenon has not been made. The authors consider that the amount of oxygen which is necessary for combustion of CO gas produced on the surface of cavity decreases because the peak position of slag foaming in the furnace becomes higher than the position of lance tip at about 6 min after the start of blowing.

3. *Outline of Blowing Reaction Model*

The following six kinds of reactions are considered as the reactions taking place in the furnace by blowing as shown in Fig. 4. Dynamic material and heat balance of these reactions are described in this model.

1) Oxidation on the surface of cavity
2) Oxidation of CO gas in the furnace
3) Slag formation
4) Reaction between slag and metal
5) Dissolution of scrap and cold metal
6) Decomposition of submaterials

Several assumptions described below have been set up so as to simplify the model.

(1) Fractions of oxygen distributed to the oxida-

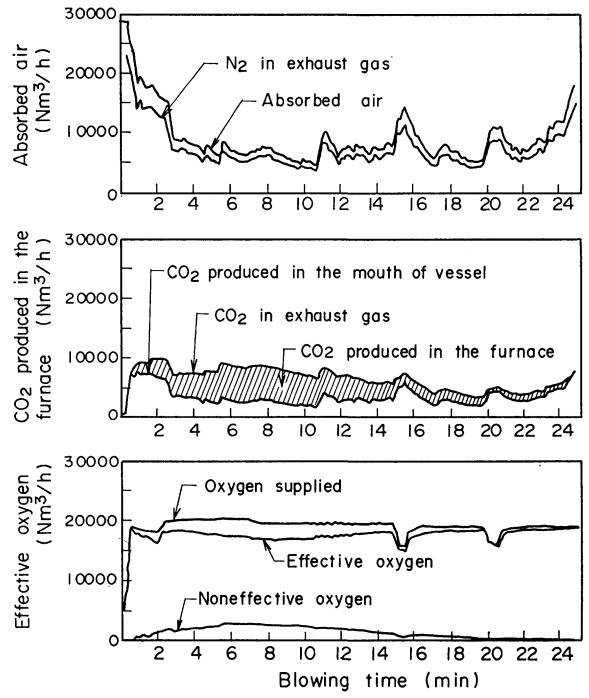

Fig. 3. Estimation of the amounts of absorbed air, CO_2 produced in the furnace, and effective oxygen.

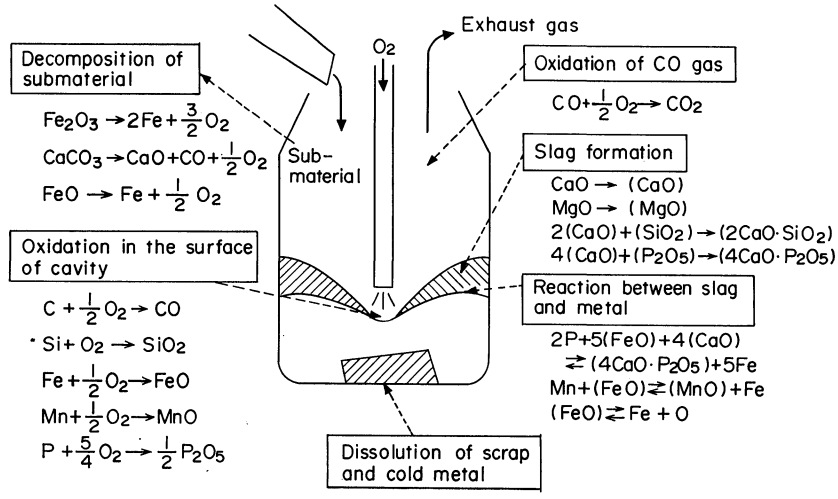

Fig. 4. Reaction process in the furnace.

tion reaction of the components of steel bath except carbon are in proportion to the product of the concentration of the component and the rate constant of oxidation.

(2) The particles of charged lime are spherical in shape, and the diameters of the particles are all the same. The melting proceeds from the surface towards the inside of the particles, and slag in contact with the particle is saturated with lime.

(3) The saturated concentration of CaO in slag can be estimated from the simplified phase diagram of the ternary (CaO)–(FeO)–(SiO_2) system.[10]

(4) For the reactions between slag and metal, the following assumptions are set up.

(i) The rates of the reactions are determined by the diffusion rates of the components of slag and metal which are taking parts of the reactions.

(ii) The equilibrium is kept at the interface of slag and metal.

(5) The heat transfer resistances in scrap and cold metal are concentrated on their surfaces.

1. Calculation of Compositions and Weight of Metal

The composition and weight of metal can be calculated by solving the dynamic equations of material and heat balance of the reactions of the above six kinds.

(1) Direct oxidation of metal components by supplied oxygen are considered to take place on the surface of cavity in molten steel as shown in Fig. 4. Muchi and Moriyama[4] calculated the fraction of oxygen distributed to the decarburization reaction through the application of the assumption (1). In this paper, the fraction of oxygen distributed to the decarburization reaction is expressed by Eq. (7) by the use of the amount of effective oxygen $V_{O_2}^{EFF}$ and the amount of oxygen consumed by decarburization $V_{O_2}^{DEC}$.

$$\sigma_c = V_{O_2}^{DEC}/V_{O_2}^{EFF} \quad \cdots\cdots(7)$$

where, σ_c: fraction of oxygen distributed to the decarburization reaction

The fractions of oxygen distributed to the oxidation reaction of metal components except carbon can be obtained by Eq. (8) on the basis of the assumption (1).

$$\sigma_i = \frac{k_i \cdot C_{im}}{\sum_j k_j \cdot C_{jm}} \cdot (1-\sigma_c) \quad \cdots\cdots(8)$$

$$i, j = \underline{\mathrm{Si}}, \underline{\mathrm{Fe}}, \underline{\mathrm{Mn}}, \underline{\mathrm{P}}$$

where, σ_i: fraction of oxygen distributed to the oxidation reaction of i-component

k_i: rate constant of the oxidation reaction of i-component (kg/kmol·s)

C_{im}: concentration of i-component in metal (kmol/kg)

The transitional variations of the concentrations of carbon and silicon in metal during blowing can be obtained as the sum of the variations due to oxidation on the surface of cavity and the quantities of components moving from scrap and cold metal into metal during dissolution.

(2) The rate of slag formation of lime can be obtained from the saturated concentration of CaO in slag according to the assumption (2).[4,10]

(3) The rates of material transfer of the components of metal and slag in the reactions between slag and metal may be expressed by Eqs. (9) and (10) on the assumption (4-i).

$$\frac{d(W_m \cdot C_{jm})}{dt} = A_m \cdot K_m \cdot \rho_m (C_{ji} - C_{jm}) \quad \cdots\cdots(9)$$

$$j = \underline{\mathrm{Mn}}, \underline{\mathrm{P}}, \underline{\mathrm{O}}$$

$$\frac{d(W_s \cdot C_{ks})}{dt} = A_m \cdot K_s \cdot \rho_s \cdot (C_{ki} - C_{ks})$$

$$k = (\mathrm{FeO}), (\mathrm{MnO}), (4\mathrm{CaO}\cdot\mathrm{P_2O_5}), (\mathrm{CaO}') \quad \cdots\cdots(10)$$

where, W_m, W_s: weights of metal and slag (kg)

C_{jm}: concentration of j-component in metal (kmol/kg)

C_{ks}: concentration of k-component in slag (kmol/kg)

C_{ji}: concentration of j-component on the interface between slag and metal (kmol/kg)

C_{ki}: concentration of k-component on the interface between slag and metal (kmol/kg)

K_m, K_s: material transfer coefficients of components in metal side and slag side (m/s)

ρ_m, ρ_s: densities of metal and slag (kg/m³)

A_m: interfacial area of slag and metal (m²)

The above (CaO′) represents an excess of base and is defined by Eq. (11).

$$C_{(\mathrm{CaO}')s} = C_{(\mathrm{CaO})s} - 2C_{(\mathrm{SiO_2})s} - 4C_{(\mathrm{P_2O_5})s} \quad \cdots\cdots(11)$$

where, $C_{(\mathrm{CaO})s}, C_{(\mathrm{SiO_2})s}, C_{(\mathrm{P_2O_5})s}$: concentrations of (CaO), (SiO_2) and (P_2O_5) in slag (kmol/kg)

The relations given by Eqs. (12) to (14) are found on the interface of slag and metal on the assumption (4-ii).

$$\frac{C_{(4\mathrm{CaO}\cdot\mathrm{P_2O_5})i}}{C_{\mathrm{P}i}^2 \cdot C_{(\mathrm{FeO})i}^5 \cdot C_{(\mathrm{CaO}')i}^4} = K_{\mathrm{P}} \quad \cdots\cdots(12)$$

$$\frac{C_{(\mathrm{MnO})i}}{C_{\mathrm{Mn}i} \cdot C_{(\mathrm{FeO})i}} = K_{\mathrm{Mn}} \quad \cdots\cdots(13)$$

$$\frac{C_{\mathrm{O}i}}{C_{(\mathrm{FeO})i}} = K_{\mathrm{FeO}} \quad \cdots\cdots(14)$$

where, $C_{\mathrm{P}i}, C_{\mathrm{Mn}i}, C_{\mathrm{O}i}$: concentrations of P, Mn, O in metal on the interface of slag and metal (kmol/kg)

$C_{(\mathrm{FeO})i}, C_{(\mathrm{MnO})i}, C_{(\mathrm{CaO}')i}, C_{(4\mathrm{CaO}\cdot\mathrm{P_2O_5})i}$: concentrations of (FeO), (MnO), (CaO′), ($4CaO \cdot P_2O_5$) in slag on the interface of slag and metal (kmol/kg)

$K_{\mathrm{P}}, K_{\mathrm{Mn}}, K_{\mathrm{FeO}}$: equilibrium constants of the reactions between slag and metal

The above K_{P}, K_{Mn}, and K_{FeO} may be calculated from

the temperature of metal. The concentrations, C_{ji} and C_{ki}, on the interface of slag and metal in Eqs. (9) and (10) can be calculated by Eqs. (12) to (14) and the stoichiometric relationships in the reactions between slag and metal.[10]

The transitional variations of the concentrations of manganese and phosphorus in metal during blowing can be obtained as the sum of the variations due to oxidation on the surface of cavity, the quantities of components moving from scrap and cold metal to metal and the variations due to the reactions between slag and metal.

(4) If heat balance and carbon balance on the surface of scrap are taken into account, the following Eqs. (15) and (16) can be obtained for dissolution of scrap.[4]

$$\alpha_{1sc}\cdot(T_m-T_{isc})=\alpha_{2sc}\cdot(T_{isc}-T_{sc})+\Delta H_{sc}\cdot\left(-\frac{dW_{sc}}{dt}\right) \quad \text{.....(15)}$$

$$\alpha_3\cdot(C_{Cm}-C_{isc})=(C_{Cm}-C_{Csc})\cdot\left(-\frac{dW_{sc}}{dt}\right) \quad \text{.....(16)}$$

where, T_m, T_{sc}: temperatures of metal and scrap (°C)

T_{isc}: temperature of metal in contact with scrap (°C)

C_{Cm}, C_{Csc}: carbon concentrations of metal and scrap (kmol/kg)

C_{isc}: carbon concentration of metal in contact with scrap (kmol/kg)

W_{sc}: weight of scrap (kg)

ΔH_{sc}: latent heat of dissolution of scrap (kcal/kg)

α_{1sc}, α_{2sc}: products of the effective surface area of scrap and the heat transfer coefficient in metal side and that in scrap side (kcal/s·°C)

α_3: product of the effective surface area of scrap and the material transfer coefficient of carbon in metal side (kg/s)

If it is assumed that the relation between temperature and carbon concentration of metal in contant with scrap is shown by the liquidus line of the iron–carbon phase diagram, the following equation can be obtained.

$$T_{isc}=\alpha_4+\alpha_5\cdot C_{isc} \quad \text{.....(17)}$$

where, α_4, α_5: constants

The above C_{isc}, T_{isc} and the dissolution rate of scrap dW_{sc}/dt can be obtained as functions of metal temperature T_m, scrap temperature T_{sc}, carbon concentration of metal C_{Cm} and carbon concentration of scrap C_{Csc} from Eqs. (15) to (17). The dissolution rate of cold metal dW_{cm}/dt can also be obtained in the same way as that for scrap dissolution.

(5) The amount of oxygen produced by decomposition of charged submaterials such as iron ore, limestone and scale is included in the amount of supplied oxygen V_{O_2} as described above. All CaO produced by decomposition of limestone is considered to be slagged in the same manner as that of charged lime.

(6) The amount of ineffective oxygen consumed by oxidation of CO gas in the furnace is calculated by the method described above.

The equations for the calculations of composition and weight of metal obtained by the above procedure are summarized in Table 1. Nomenclature used in Table 1 is as follows:

W_{cm}, $W_{(FeO)}$: weights of cold metal and (FeO) in slag (kg)

$V^E_{O_2}$: amount of effective oxygen (kmol/s)

C_{Ccm}, C_{Sicm}, C_{Mncm}, C_{Pcm}: concentrations of C, Si, Mn and P in cold metal (kmol/kg)

C_{Csc}, C_{Sisc}, C_{Mnsc}, C_{Psc}: concentrations of C, Si, Mn and P in scrap (kmol/kg)

M_j: atomic weight of component j (kg/kmol)

M_{Fe}: atomic weight of Fe (kg/kmol)

M_{FeO}: molecular weight of FeO (kg/kmol)

W_{SUB}: weight of charged submaterials (kg)

k_{SUB}: constant.

2. Calculation of Temperature of Metal

The changes in heat energies of metal and slag

Table 1. Equations used for the calculation of composition and weight of metal.

Item		Equations
Composition	C	$\frac{d(W_m\cdot C_{Cm})}{dt}=-\sigma_C\cdot V^E_{O_2}+C_{Ccm}\cdot\left(-\frac{dW_{cm}}{dt}\right)+C_{Csc}\cdot\left(-\frac{dW_{sc}}{dt}\right)$
	Si	$\frac{d(W_m\cdot C_{Sim})}{dt}=-\frac{\sigma_{Si}}{2}\cdot V^E_{O_2}+C_{Sicm}\left(-\frac{dW_{cm}}{dt}\right)+C_{Sisc}\left(-\frac{dW_{sc}}{dt}\right)$
	Mn	$\frac{d(W_m\cdot C_{Mnm})}{dt}=-\sigma_{Mn}\cdot V^E_{O_2}+C_{Mncm}\left(-\frac{dW_{cm}}{dt}\right)+C_{Mnsc}\left(-\frac{dW_{sc}}{dt}\right)+A_m\cdot K_m\cdot\rho_m(C_{Mni}-C_{Mnm})$
	P	$\frac{d(W_m\cdot C_{Pm})}{dt}=-\frac{2}{5}\sigma_P\cdot V^E_{O_2}+C_{Pcm}\left(-\frac{dW_{cm}}{dt}\right)+C_{Psc}\left(-\frac{dW_{sc}}{dt}\right)+A_m\cdot K_m\cdot\rho_m(C_{Pi}-C_{Pm})$
Weight		$\frac{dW_m}{dt}=-(1-\Sigma M_j\cdot C_{jcm})\cdot\frac{dW_{cm}}{dt}-(1-\Sigma M_j\cdot C_{jsc})\frac{dW_{sc}}{dt}+\Sigma M_j\cdot\frac{d(W_m\cdot C_{jm})}{dt}-\frac{M_{Fe}}{M_{FeO}}\cdot\frac{dW_{(FeO)}}{dt}+\Sigma k_{SUB}\frac{dW_{SUB}}{dt}$
		j=C, Si, Mn, P

may be calculated, on the assumption that heat energies such as heat losses through the furnace wall and throat, heat transfer to exhaust gas and heat exchange between slag and metal besides the heats of reactions, dissolution and decomposition in the process shown in Fig. 4 are distributed to metal and slag in fixed proportions, respectively. The values of the proportions a_i and b_i are determined by the analysis of the actual operational data. The changes in heat energies of scrap and cold metal may be obtained from heat balance of scrap and cold metal.[4]

The equations for the calculations of temperatures of metal and slag obtained by the above method are as follows:

$$\frac{d(c_p \cdot W_m \cdot T_m)}{dt} = \sum_{i=1}^{10} a_i \cdot Q_i \quad \text{.....(18)}$$

$$\frac{d(c_{ps} \cdot W_s \cdot T_s)}{dt} = \sum_{i=1}^{10} b_i \cdot Q_i \quad \text{.....(19)}$$

where, Q_1: heat of oxidation on the surface of cavity (kcal/s)
Q_2: heat of slag formation (kcal/s)
Q_3: heat of reaction between slag and metal (kcal/s)
Q_4: heat of oxidation of CO gas in the furnace (kcal/s)
Q_5: heat of dissolution of cold metal and scrap (kcal/s)
Q_6: heat of decomposition of submaterials (kcal/s)
Q_7: heat loss through the furnace wall (kcal/s)
Q_8: heat loss through the furnace throat (kcal/s)
Q_9: heat exchange between slag and metal (kcal/s)
Q_{10}: heat transfer to exhaust gas (kcal/s)
c_p, c_{ps}: specific heats of metal and slag (kcal/kg·°C)
T_s: temperature of slag (°C).

4. *Method of Numerical Calculation*

The equations used for the calculations on the basis of the blowing reaction model described in *Sec. II. 3* can be expressed by nineteen differential equations and six algebraic equations as shown in Eqs. (20) and (21).

$$\dot{y}_i = f_i(y_1, y_2, \ldots, y_{19}, y_{20}, \ldots, y_{25}) \quad i = 1, 2, \ldots, 19 \quad \text{.....(20)}$$

$$g_j(y_1, y_2, \ldots, y_{19}, y_{20}, \ldots, y_{25}) = 0 \quad i = 20, 21, \ldots, 25 \quad \text{.....(21)}$$

Variables, y_i, in the above equations represent the concentrations of C, Si, Mn, P and O in metal, the concentrations of (SiO_2), (FeO), (MnO), (P_2O_5), (CaO) and (MgO) in slag, the weights of metal, slag, scrap and cold metal, and temperatures of metal, slag, scrap and cold metal. Variables y_j represent the saturated concentration of CaO,[10] the concentrations of P, Mn and O on the interface of slag and metal,[10] and the temperature of metal in contact with cold metal and scrap. Equations (20) and (21) have been solved at every 10 s interval by means of Runge–Kutta method and Newton–Raphson method. Before being solved Eq. (20), the values of variables $y_{20}, y_{21}, \ldots, y_{25}$ in the right hand side of Eq. (20) are determined by substituting the calculated values of variables $y_1, y_2 \ldots, y_{19}$ into Eq. (21). In the calculation of the amount of effective oxygen $V_{O_2}^{EFF}$ and the amount of oxygen $V_{O_2}^{DEC}$ consumed by the decarburization reaction, the exhaust gas analysis data at 20 s before the feed is used because the delay time of exhaust gas, that is, 20 s is taken into consideration.

The above model includes the parameters such as the rate constants in the oxidation reaction on the surface of cavity, the material transfer coefficients in the reactions between slag and metal and the proportions of heat energies distributed to metal and slag. The values of these parameters are determined so as to obtain good agreement between the calculated values and the measured values of metal composition, metal temperature and slag composition. As for the rate constants of oxidation on the surface of cavity, $K_{Si}=10\times10^{12}$ (kg/kmol·s), $k_{Fe}=0.0133\times10^{12}$ (kg/kmol·s), $k_{Mn}=1\times10^{12}$ (kg/kmol·s) and $k_P=10\times10^{12}$ (kg/kmol·s) are obtained.

5. *Correction for Flow Rate of Exhaust Gas*

The measured values by Venturi type of flow meter are used as the flow rates of exhaust gas in the model. In this case, the errors inherent in the measurement of flow rate due to dust adhesion and so on can not be neglected. The sum of the amount of CO produced by decarburization and CO produced by decomposition of charged submaterials are equal to the sum of the amounts of CO and CO_2 in the exhaust gas. Therefore the estimated values of the former are influenced by the experimental errors of exhaust gas flow rate. Correction coefficient expressed by Eq. (22) for the flow rate is introduced to compensate the experimental errors.

$$K_G = [(W_m^0 \cdot C_{Cm}^0 + W_{cm}^0 \cdot C_{Ccm} + W_{sc}^0 \cdot C_{Csc} - W_m^E \cdot C_{Cm}^E) \times 22.4 + \sum V_{CO}^{SUB}] / \sum (V_{CO}^{EX} + V_{CO_2}^{EX}) \quad \text{.....(22)}$$

where, K_G: extent of deviation due to the experimental errors of exhaust gas flow rate
W_m^0, W_{cm}^0, W_{sc}^0: initial weights of metal, cold metal and scrap (kg)
C_{Cm}^0: initial concentration of carbon in metal (kmol/kg)
C_{Cm}^E: actual endpoint concentration of carbon in metal (kmol/kg)
W_m^E: actual end point weight of metal (kg)

The symbol $\sum$ represents the sum from the start of blowing to the end of blowing. The flow rates of exhaust gas in the actual operation are corrected as Eq. (23) with the average $\bar{K}_G$ of K_G calculated from Eq. (22).

$$V_{EX}^R = \bar{K}_G \cdot V_{EX} \quad \text{.....(23)}$$

where, V_{EX}: measured flow rate of exhaust gas (Nm^3/h)

$\bar{K}_G$: correction coefficient for the flow rate of exhaust gas

V^R_{EX}: corrected flow rate of exhaust gas (Nm^3/h)

Figure 5 shows the change in correction coefficient for the flow rate of exhaust gas at one campaign. It is confirmed that $\bar{K}_G$ decreases because the amount of adhering dust increases as the number of heats increases.

6. *Adaptive Modification of Parameters in the Model*

The composition and temperature of metal may be estimated by the above-mentioned model, but the following adaptive modification is made with the actual data at the end point of blowing to deal with the variation of operational condition. The concentrations of carbon and phosphorus and temperature of metal are significant as the objects of estimation. In this study, the material transfer coefficient K_m of the component in metal for the reaction between slag and metal as for the phosphorus concentration, and the proportion a_7 of the heat loss through the furnace wall distributed to metal regarding metal temperature are chosen as the parameters which should be modified adaptively. These parameters are modified adaptively so as to obtain good agreement between the calculated and the actual values of phosphorus concentration and temperature at the end point. For the carbon concentration of metal, a decrease in the estimation accuracy can be prevented by making correction for the flow rate of exhaust gas.

III. *Verification of Validity of the Mathematical Model*

1. *Simulation Example by the Model*

The results of numerical calculations are shown in Figs. 6 to 10. Figure 6 shows the transitional changes in fraction of oxygen distributed on the surface of cavity. It is confirmed that a greater part of effective oxygen in consumed by oxidation of silicon in metal in the first stage of blowing and almost all the effective oxygen is consumed by decarburization in the middle stage of blowing after the removal of silicon from metal. Figure 7 shows the transitional changes in weights of metal, slag and scrap. Figure 8 shows the calculated value of the transitional changes in composition and temperature of metal compared with the actual data measured by a sub-lance. The estimation accuracy of composition and temperature of metal is fair except the behavior of manganese in the middle stage of blowing. The temperature gradient is much larger in the final stage than that in the middle stage of blowing as shown in Fig. 8. The reason is considered to be that dissolution of scrap is finished as shown in Fig. 7 and that oxidation of iron in metal is accelerated as shown in Fig. 6 in the final stage of blowing. Figure 9 shows the transitional change in weight of slag. Figure 10 shows the calculated value of the transitional change in slag composition compared with the actual data measured at the end point. It is found from Fig. 10 that the calculated values

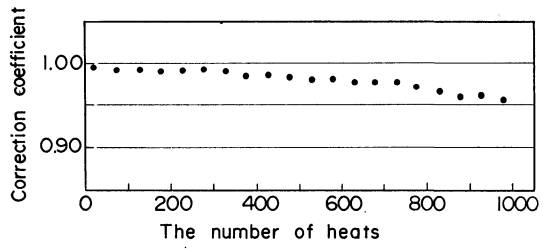

Fig. 5. The change in correction coefficient for the flow rate of exhaust gas.

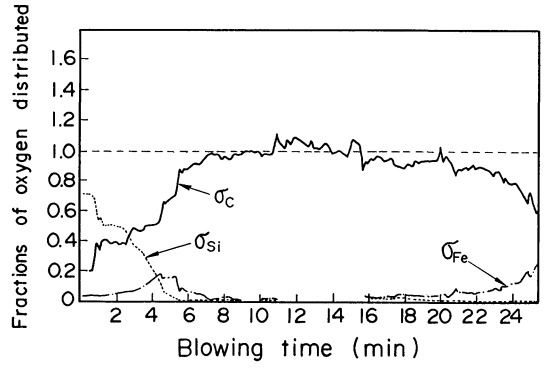

Fig. 6. Estimation of the fraction of oxygen distributed on the surface of cavity.

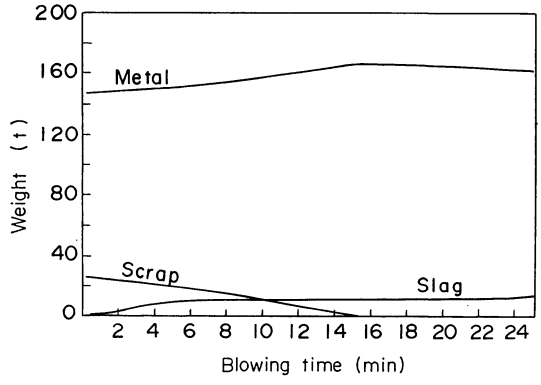

Fig. 7. Estimation of the amounts of metal, slag and scrap.

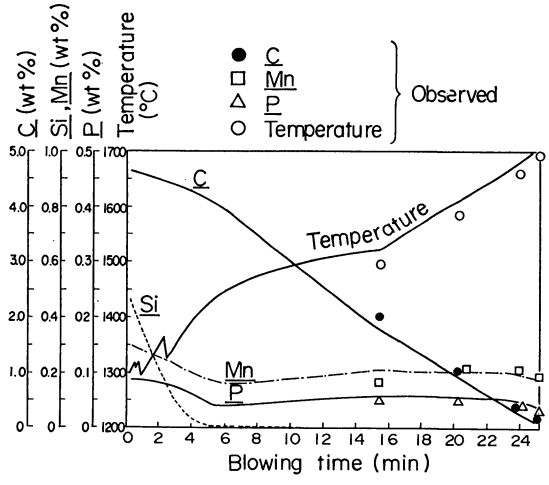

Fig. 8. Estimation of the composition and temperature of steel bath.

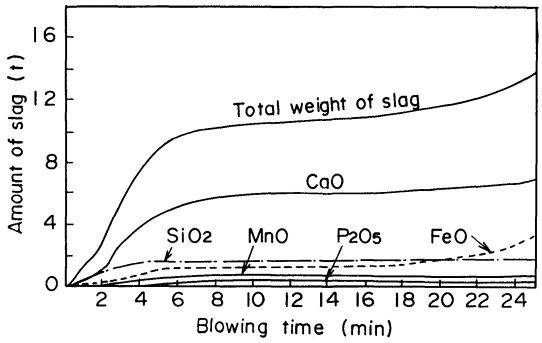

Fig. 9. Estimation of the amount of slag.

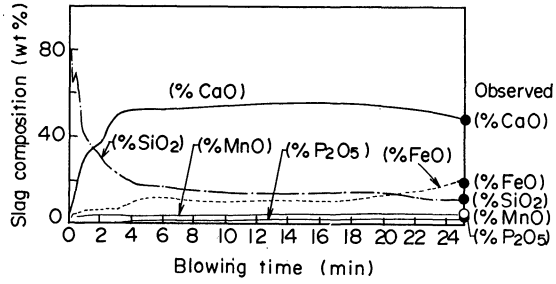

Fig. 10. Estimation of the slag composition.

agree well with the measured slag compositions at the end point. Accuracy of the estimation of carbon and phosphorus concentrations and the temperature of metal at the end point of blowing made by the use of operational data are better than ±0.05 %, ±0.01 % and ±20°C, respectively.

2. *Trajectory Modification Based on Sub-lance Measurement*

In the acutal operation, the carbon concentration and the temperature of metal are measured with a sub-lance in the final stage of blowing. Therefore the estimated carbon concentration and the estimated temperature may be replaced by the actual values measured with a sub-lance as expressed in Eqs. (24) and (25).

$$C_{Cm} = C_{CSL} \quad \text{.....(24)}$$

$$T_m = T_{mSL} \quad \text{.....(25)}$$

where, C_{CSL}: carbon concentration of metal measured with a sub-lance (kmol/kg)

T_{mSL}: temperature of metal measured with a sub-lance (°C)

However, such a replacement has not been made because the sub-lance measurement is not normal when there is a large difference between the values measured with a sub-lance and the calculated ones. Figure 11 shows the calculated results with trajectory modification by Eqs. (24) and (25).

IV. Conclusion

Studies on the end point control of the BOF steelmaking process have been made to mainly control the carbon content and the temperature of molten steel. Controls of the phosphorus and manganese contents

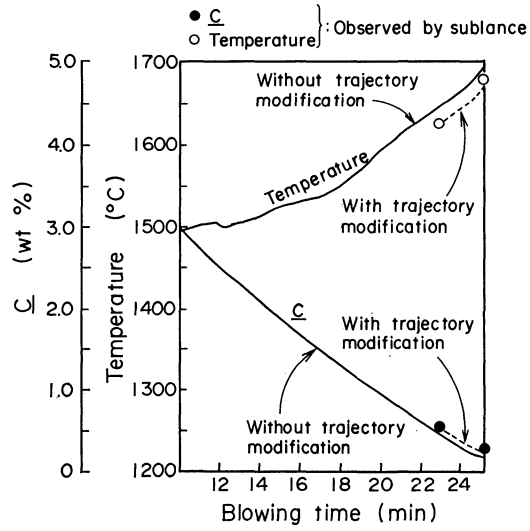

Fig. 11. Trajectory modification based on the sub-lance measurement.

are now being investigated. In this paper, for the purpose of understanding quantitatively the transition of composition including the phosphorus and manganese contents and the temperature of steel bath during blowing, a mathematical model, being able to use for the on-line application to BOF, has been established, and the results obtained are summarized as follows:

(1) By the use of the amounts of blown oxygen and charged submaterials and the composition and flow rate of gas exhausted from BOF as the result of reactions in the furnace, the amounts of effective oxygen consumed by oxidation on the surface of cavity of molten steel and of oxygen consumed by decarburization have been determined.

(2) By including the calculated amount of oxygen in the blowing reaction model based on the reaction theory, the transition of composition including the phosphorus and manganese contents and the temperature of steel bath have been estimated.

The mathematical model established in the present work has been applied to No. 1 BOF shop in Wakayama Steel Works. It has been used as the guide of the operation and has contributed to the reduction of reblow ratio.

Acknowledgements

The authors wish to express their thanks to the late Dr. I. Muchi, Professor of the Faculty of Engineering, Nagoya University, and to Dr. S. Asai, Assistant Professor of the Faculty of Engineering, Nagoya University, for their guidance and suggestions for the present research work.

REFERENCES

1) Y. Takemura, K. Kato and S. Fukuda: *Seitetsu Kenkyu*, (1977), No. 291, 12.
2) T. Ohta, M. Saigusa, J. Nagai, F. Sudo, K. Nakanishi, T. Nozaki and R. Uchimura: *Kawasaki Steel Tech. Rep.*, **12** (1981), 209.
3) T. Takawa, Y. Misaka, K. Katayama, H. Tsujikawa and

K. Sakuraba: *Tetsu-to-Hagané*, **66** (1980), S766; *Trans. Iron Steel Inst. Jpn.*, **21** (1981), B207.
4) I. Muchi and A. Moriyama: Yakin Hannou Kogaku, Yokendo, Tokyo, (1972), 270.
5) K. Taguchi, A. Ozeki, T. Hasegawa, T. Shiratani, I. Tsuboi and K. Matsui: *Tetsu-to-Hagané*, **63** (1977), A95.
6) I. Tanaka, Y. Jyono, M. Kanemoto, T. Yoshida, Y. Ueda and K. Isogami: *Tetsu-to-Hagané*, **66** (1980), S768; *Trans. Iron Steel Int. Jpn.*, **21** (1981), B122.
7) Y. Iida, K. Emoto, M. Ogawa, M. Onishi and H. Yamada: *Tetsu-to-Hagané*, **68** (1982), 2480.
8) Y. Nimura, T. Hasegawa, M. Hanmyo, Y. Miyawaki and T. Usui: *Tetsu-to-Hagané*, **69** (1983), S1003.
9) T. Takawa, K. Katayama, K. Katohgi, Y. Enomoto and Y. Murazawa: *Tetsu-to-Hagané*, **69** (1983), S205.
10) M. Miwa, S. Asai and I. Muchi: *Tetsu-to-Hagané*, **56** (1970), 1677.